Hindawi
Advances in Civil Engineering
Volume 2019, Article ID 2706976, 12 pages
https://doi.org/10.1155/2019/2706976

Research Article

Statistical Analysis of Influence of Cover Depth on Loess Tunnel Deformation in NW China

Zhao Hu, Ke Du, Jinxing Lai, and Yongli Xie

School of Highway, Chang'an University, Xi'an 710064, China

Correspondence should be addressed to Jinxing Lai; laijinxing@chd.edu.cn

Received 28 September 2018; Accepted 18 November 2018; Published 3 February 2019

Academic Editor: Emanuele Brunesi

Loess is a kind of special soil with structure and hydrocollapse behavior; due to the particularity of loess, the deformation regularity of the tunnel in loess shows different characteristics from those in rock. To ensure the safety of construction, crown settlement (CS) and horizontal convergence (HC) are widely used to assess the stability of the tunnel structural system. Based on statistical analysis, this study focused on analyzing the influence of cover depth on the deformation of surrounding rock of loess tunnels by ANOVA, and relationships between them were presented by regression analysis. The achieved results indicated that the influence of cover depth on deformation was not obvious in shallow tunnels, while the cover depth had a significant effect on deformation in deep tunnels. Based on the difference of influence of cover depth on deformation between shallow tunnels and deep tunnels, a method for determining the cover depth threshold (CDT) in the tunnel by statistical analysis was proposed. The horizontal and vertical deformations in shallow tunnels were discrete and obeyed the positive distribution, mainly concentrated within 200 mm. The deformation allowance in shallow tunnels was recommended to be 200 mm. In deep tunnels, as the cover depth increased, the deformation increased linearly, while the CS/HC decreased.

1. Introduction

Loess is widely distributed and accounts for 1/6 of China territory as shown in Figure 1 [1], necessitating the construction of tunnels in loess regions. In recent years, several roads have been built in loess areas in China (e.g., Zhengzhou–Xi'an High-Speed Railway (2010), Yan'an–Xi'an Highway (2016), Baoji–Lanzhou High-Speed Railway (2017), and Datong–Xi'an High-Speed Railway (2021)). Therefore, loess tunnels are springing up in the loess regions of China [2, 3]. China loess is characterized by structure, macroporous loess, low plasticity indices, low moisture content, short-range bonds, and decreasing the shear strength upon saturation [4–11].

Due to the particularity of loess, the deformation regularity in loess tunnels shows different characteristics from those in rock tunnels [12–17]. Deformation has four characteristics: scientific, timeliness, reliability, and convenience, and is widely used to evaluate tunnel stability and ensure construction safety [18–25]. The deformation of surrounding rock in loess is mainly affected by water content, cover depth, construction method, and construction procedure [26]. During the tunnel construction in loess ground, the sequential excavation method (SEM) is widely applied to promote the tunnel face stability, such as both-side drift method (BSDM), bench excavation method (BEM), central diaphragm method (CD), and cross diaphragm method (CRD), as shown in Figure 2. The BEM is adopted in the regions with ordinary surrounding rock, while the CD and CRD are mainly used in the sections with weathering rock, poor geology, or tunnel portal. SEM is very effective in controlling deformation. The deformation undergoes expansion and stabilization stages and needs longer time for stability. With passing the time, the surrounding rock gradually tends to be stable, and the stability time of surrounding rock is different under different grades [27–29]. The crown would create the whole settlement after excavation, and the differential settlement is little between the crown and the walls [30–33]. In addition, the deformation of crown settlement (CS) is greater than that of horizontal convergence (HC). When the initial support is closed into rings, the displacement around the

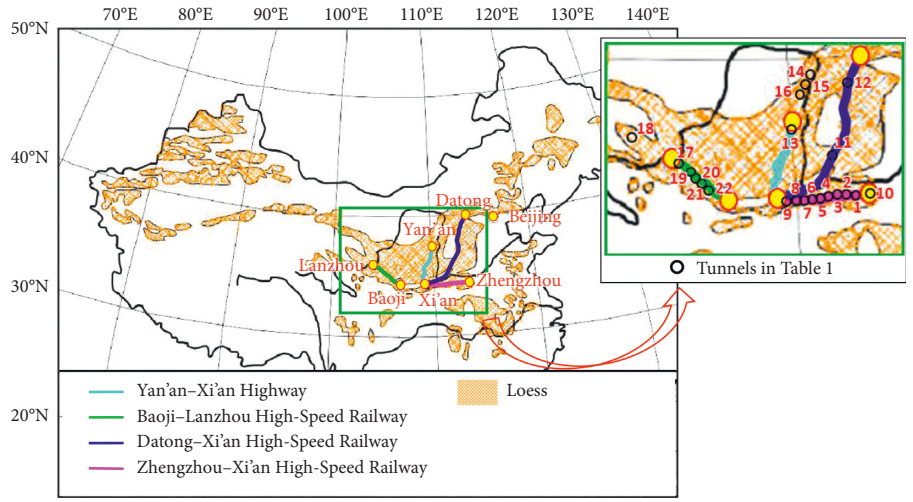

Figure 1: Outline of major loess deposits in China [1].

(a) (b) (c) (d)

Figure 2: Excavation methods (number is excavation order). (a) BEM. (b) BSDM. (c) CRD. (d) CD.

tunnel would not increase any longer [34, 35]. The ultimate deformation of loess tunnels is larger than that of the general soil tunnels, and the large deformation reflects the weakness of the primary support of structure [36]. Due to the lack of comprehensive research methods, the understanding of loess deformation regularity is still insufficient so the deformation trend with time is often used to evaluate tunnel stability [37–40].

Cover depth is the distance from the crown of tunnel to the ground [41]. Based on engineering experience, cover depth is used to choose calculation methods of surrounding rock pressure and is one of the major factors affecting the deformation of surrounding rock [42–45]. Statistical analysis, as an important approach to study regularity, is widely used to analyze monitoring data of deformation in rock tunnels, whereas rarely in loess tunnels [46–48]. This paper studies the influence of cover depth on the deformation of surrounding rock of loess tunnels by ANOVA and relationships between them were presented by regression analysis, providing a more reliable theoretical basis for the deformation law of surrounding rock in the design and construction of loess tunnels.

2. Methodology

The deformation processing was different between BEM and those with the temporary support sidewall (CRD, CD, BSDM, etc.). Thus, only the statistical data made up of CS and HC basing on BEM was analyzed [49, 50]. The settlement and convergence monitoring points by BEM are shown in Figure 3.

The data of the 22 tunnels used in this paper were from the papers of Zhao et al. [51], Hu [36], and Li et al. [26]. Table 1 and Figure 1 showed an overview of the part loess tunnel, which was published on journals or monographs publicly. To eliminate the influence of the difference of sandy loess and clayey loess on the deformation results, the research objects were all sandy loess. Finally, the data of 62 sections would be analyzed. Grouping and classifying at the level of effective factors, the data are listed in Table 2.

The deformation data classified by approximate depth and span have 4 spans and 8 depth levels. The data of Table 2 are count in accordance with the two factors cover depth and span, and the result is presented in Table 3. The analysis of variance (ANOVA) was used to study whether the tunnel deformation was significantly different at different levels under specific spans, to study whether the influence of cover depth on deformation was significant. The probability of 0.05 and the corresponding F value were used to determine the significance. When the influence of cover depth on deformation was not significant, the distribution characteristics of the deformation would be studied. When the influence was significant, regression analysis would be used to predict the function relationship between depth and deformation. In the regression analysis, the linear equation was used to predict the influence of single factor on the deformation. Figure 4 displayed the statistical analysis procedure.

SPSS was used for statistical analysis.

Steps of ANOVA:

(1) Establish test hypothesis.

  (i) H0: the mean values of the cover depth levels are equal
  (ii) H1: the mean values of the cover depth levels are not equal or incomplete
  (iii) The test level is 0.05

(2) Calculate the F value

(3) Determine the P value and make an inference result

Steps of the regression analysis:

(1) According to the data of cover depth and deformation, the regression equation is initially set

(2) Solving regression coefficient

(3) Perform a correlation test and determine the correlation coefficient

(4) After meeting the relevant requirements, the regression equation and the specific conditions can be combined to determine the trend of the deformation with the cover depth, and the confidence interval of the predicted value can be calculated

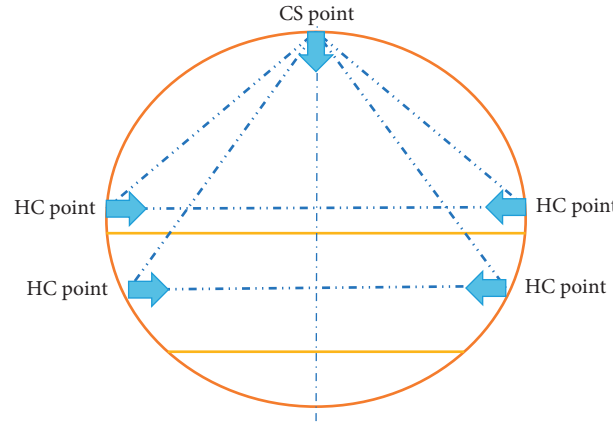

Figure 3: Tunnel deformation monitoring by BEM.

3. ANOVA and Significance Test

3.1. Significance Analysis between Deformation and Cover Depth at 15.2 m Span. Figure 5 showed the statistical results of mean of deformation on CS and HC. There were great differences in deformation under different span and depth. All deformations were within 250 mm.

Figure 6 and Table 4 listed the results of the ANOVA. For CS, when the difference in cover depth was 10 m and 32 m, the probability that the deformation was at the same level was $P = 0.312 > 0.05$ and $F = 1.13 < F$ crit $= 4.96$. At these cover depth levels, there was no significant difference in deformation. However, when the cover depth was at 32 m, 95 m, 110 m, and 175 m, and the probability that the deformation was at the same level was $P \leq 0.001 < 0.05$ and $F = 17.74 > F$ crit $= 2.99$. At these cover depth levels, there was significant difference in deformation.

For HC, when the cover depth was at 32 m, 95 m, 110 m, and 175 m, the probability that the deformation was at the same level was $P \leq 0.001 < 0.05$ and $F = 34.63 > F$ crit $= 3.03$. At these cover depth levels, there was significant difference in deformation.

When the cover depth was less than 32 m, the influence of the cover depth on the deformation was not significant. While the cover depth changed from 32 m to 175 m, the variation of the cover depth had a significant influence on the deformation.

3.2. Significance Analysis between Deformation and Cover Depth at 12.26 m Span. Figure 6 and Table 4 listed the results of the ANOVA. For CS, when the difference in cover depth was 10 m and 32 m, the probability that the deformation was at the same level was $P = 0.445 > 0.05$ and $F = 0.77 < F$ crit $= 10.13$. At these cover depth levels, there was no significant difference in deformation. However, when the cover depth was at 45 m and 100 m, the probability that the deformation was at the same level was $P = 0.019 < 0.05$ and $F = 8.12 > F$ crit $= 5.12$. At these cover depth levels, there was significant difference in deformation.

For HC, when the difference in cover depth was 10 m and 32 m, the probability that the deformation was at the

Table 1: Overview of part loess tunnels [26, 36, 51].

Number	Tunnel	Loess types	Span (m)	Excavation method
1	Zhangmao	Q2 CL	15.2	BEM
2	Hejiazhuang	Q2 CL	15.2	BEM
3	Hanguguan	Q3 SL	15.2	CRD and BEM
4	Wenxiang	Q2 CL	15.2	BSDM
5	Pandong	Q3 SL	15.2	CRD
6	Taicun	Q3 SL	15.2	CRD
7	Qindong	Q3 SL, Q1 CL, Q1 SL	15.2	BSDM + BEM
8	Tongluochuan	Q3 SL, Q1 CL, Q1 SL	15.2	CRD and CD
9	Gaoqiao	Q3 SL, Q2 SL	15.2	BEM
10	Taohuayu	Q2 SL	17.3	BEM
11	Xixian	Q2 CL	12.2	BEM
12	Yuanyanghui	Q3 SL	12.2	BEM
13	Qingpita	Q3 SL	12.2	BEM
14	Mizhi number 1	Q3 SL	12.77	BEM
15	Dunliang	Q2 CL	17.31	BEM
16	Liujiaping	Q2 CL	12.26	BEM
17	Humaling	Q3 SL	13.6	BEM
18	Dayushan	Q3 SL	12.2	BEM
19	Nanershilipu	Q3 SL	15.2	BEM
20	Anding	Q3 SL	15.2	BEM
21	Sujiachuan	Q3 SL	15.2	BEM
22	Wangjiagou	Q3 SL	15.2	BEM

Q_2: Middle Pleistocene. Q_3: Late Pleistocene. SL: sandy loess. CL: clayey loess. BSDM: both-side drift method. BEM: bench excavation method. CD: central diaphragm method. CRD: cross diaphragm method.

same level was $P = 0.688 > 0.05$ and $F = 0.18 < F$ crit $= 6.61$. At these cover depth levels, there was no significant difference in deformation. However, when the cover depth was at 45 m and 100 m, the probability that the deformation was at the same level was $P = 0.003 < 0.05$ and $F = 14.98 > F$ crit $= 4.96$. At these cover depth levels, there was significant difference in deformation.

When the cover depth was less than 45 m, the influence of the cover depth on the deformation was not significant. While the cover depth changed from 45 m to 100 m, the variation of the cover depth had a significant influence on the deformation.

3.3. Discussions on ANOVA. It could be seen from the results of ANOVA that the change of the cover depth on the deformation had no significant influence in the shallow tunnels, while had a significant influence on the deep tunnels. In deep tunnels and shallow tunnels, cover depth had different effects on deformation.

This was because the surrounding rock pressure in the shallow tunnel was dominated by loose surrounding rock pressure, and the loose pressure had a large dispersion, which means that the tunnel deformation was random with the change of cover depth. While in the deep tunnel, the surrounding rock pressure was mainly deformation pressure. And in the shallow crust less than 500 m, the vertical stress was dominated by the rock mass and increased linearly with the increase of cover depth. This characteristic of the surrounding rock pressure was manifested by a linear increase in deformation as the depth increased [52, 53].

Due to the difference of surrounding rock pressure between shallow tunnels and deep tunnels, different calculation methods were used in tunnel structure calculations [41]. And the depth used to determine whether a tunnel is a deep tunnel or a shallow tunnel is called cover depth threshold (CDT).

According to the difference of the significance level of cover depth to the deformation of deep tunnel and shallow tunnel, a method for determining the CDT by using the statistical method was proposed. When cover depth had no significant effect on deformation, it was a shallow tunnel. When cover depth had a significant effect on deformation, it was a deep tunnel.

4. Regression Analysis

According to the ANOVA, the deformation of surrounding rock of the loess tunnel was related to cover depth. To find the relationship between the deformation of the surrounding rock and cover depth, further regression analyses were needed. Linear regression is extensively used in regression analysis and is the major method. Firstly, the scatter plot of surrounding rock deformation with influencing factors was proposed. Then, the estimated relationship could be obtained. Finally, the hypothesis test would be used to determine if the function relation was appropriate.

4.1. Regression Analysis between Deformation and Cover Depth at 15.2 m Span

4.1.1. Linear Regression between CS and Cover Depth at 15.2 m Span. Figure 7 shows the scatter plot between CS and cover depth at 15.2 m span. It demonstrated that the CS increased as the cover depth increased. Considering the linear trend, the linear correlation coefficient was 0.616, and the regression equation is as follows:

Table 2: Data of deformation.

Cover depth (m)	Span (m)	CS (mm)	HC (mm)
10	6.2	11.88	5.95
10	6.2	11.55	5.82
10	15.2	93	—
10	15.2	168	—
32	12.26	13	15
32	12.26	—*	12
32	12.26	14	18.3
32	15.2	87	—
32	15.2	72	—
32	15.2	—	45
32	15.2	—	36
32	15.2	92	50
32	15.2	80	37
32	15.2	157	60
32	15.2	151	56
32	15.2	103	54
32	15.2		62
32	15.2	80	44
32	15.2	101	24.85
45	12.26	18.39	10.08
45	12.26	11	12
45	12.26	32	10
45	12.26	—	22
90	17.31	98.4	118
90	17.31	105	113
90	17.31	98	–
90	17.31	107.6	116.6
90	17.31	106.4	100.8
90	17.31	119.2	122.4
90	17.31	110.2	124
90	17.31	74	146.4
90	17.31	63	133.4
90	17.31	86	138.4
90	17.31	77	143.2
95	15.2	67	60
95	15.2	83	65
95	15.2	59	57
95	15.2	75	59
100	12.26	166.6	277.3
100	12.26	171	222.8
100	12.26	228.4	274.2
100	12.26	165	179.4
100	12.26	200.6	164.6
100	12.26	71.2	107.2
100	12.26	56.8	87
100	12.26	49.8	73.6
110	15.2	150	105
110	15.2	146	54
110	15.2	147	60
110	15.2	143	40
110	15.2	155	86
110	15.2	159	66
110	15.2	131	29
110	15.2	145	—
175	15.2	111	167
175	15.2	95	119
175	15.2	94	149
175	15.2	98	151
175	15.2	77	126
175	15.2	120	—
195	15.2	124	158
210	15.2	219	289

*indicates no data.

$$y_{CS} = (0.358x + 37.335) \times 10^{-3}. \quad (1)$$

t-test was used for hypothesis testing H_0: $\beta_1 = 0$. The results were $t^* = 3.046 > t\ (0.05) = 2.365$ and P value $= 0.019 < 0.05 = \alpha$. There was a sufficient evidence at the 0.05 significance level to conclude that there was a linear relationship in the population between the cover depth and CS.

4.1.2. Linear Regression between HC and Cover Depth at 15.2 m Span. Figure 8 shows the scatter plot between HC and cover depth at 15.2 m span. It showed that the HC increased as the cover depth increased. Considering the linear trend, the linear correlation coefficient was 0.830, and the regression equation is as follows:

$$y_{HC} = (1.095x - 43.793) \times 10^{-3}. \quad (2)$$

t-test was used for hypothesis testing H_0: $\beta_1 = 0$. The results were $t^* = 9.5 > t\ (0.05) = 2.447$ and P value $= \leq 0.001 < 0.05 = \alpha$. There was sufficient evidence at the 0.05 significance level to conclude that there was a linear relationship in the population between the cover depth and HC.

4.1.3. Regression Analysis between CS/HC and Cover Depth at 15.2 m Span. To take in further analysis of the relation between deformation and cover depth, the characteristic of the data on the CS/HC from the on-site and the equation was explored. The equation of the CS/HC varying with cover depth could be obtained by the fitting equation (1) CS and equation (2) HC. The new function is as follows:

$$y_T = \left(\frac{y_{CS}}{y_{HC}}\right) = \frac{(0.358x + 37.335)}{(1.095x - 43.793)}. \quad (3)$$

Equation (3) was fitted with the function being similar in form of $y = a + b/(c + x)$. Nonlinear regression was carried out with SPSS software package, and the fitting equation was obtained as follows:

$$y_R = \frac{0.003 + 111.092}{(x - 0.169)}. \quad (4)$$

When the span was 15.2 m, the cover depth varied from 90 to 175 m, comparing the graph of equation (3) regarded as theoretical curve and equation (4) regarded as regression curve, and the result is plotted in Figure 9. When the cover depth was below 90 m, the difference between the two curves

Table 3: Distribution of data on cover depth and span.

Span	Cover depth							
	10	32	45	90	95	100	110	175
6.2	2*	—**	—	—	—	—	—	—
12.26	—	3	4	—	—	8	—	—
15.2	2	12	—	—	4	—	8	6
17.3	—	—	—	11	—	—	—	—

*indicates there are 2 data when the cover depth is 10 m and the span is 6.2 m. **indicates no data when the cover depth is 32 m and the span is 6.2 m.

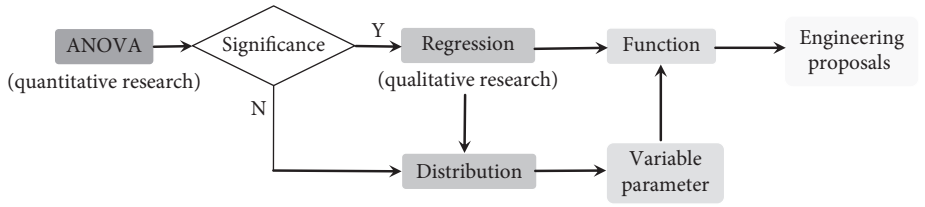

Figure 4: Approach of the statistical analysis.

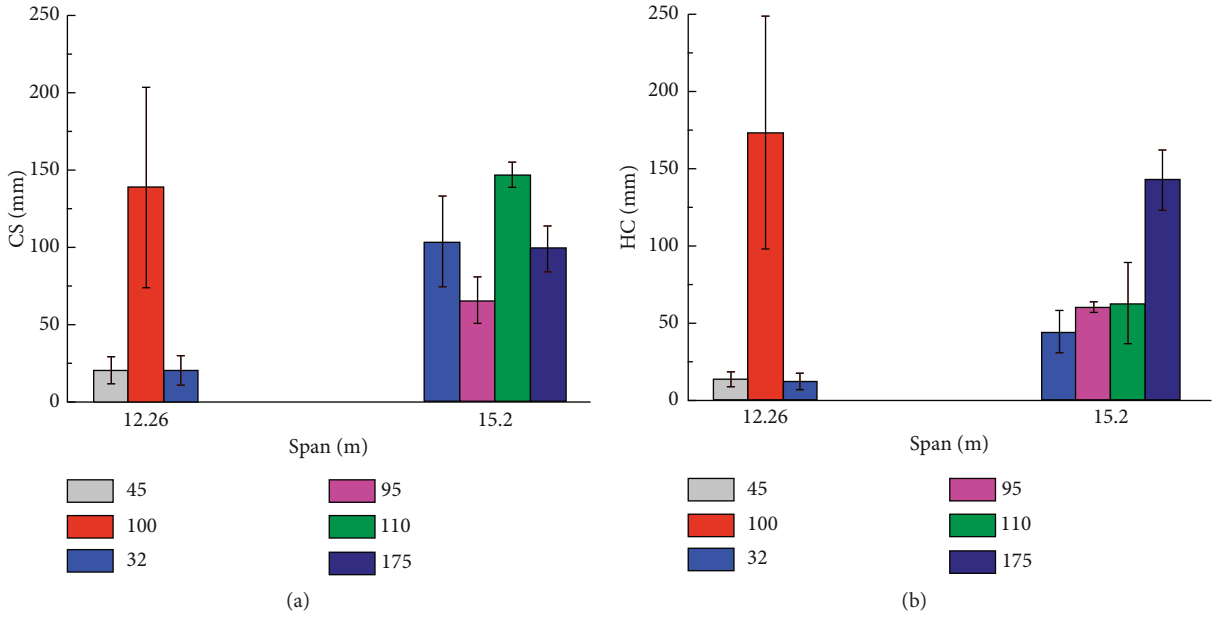

Figure 5: Variation of deformation with cover depth.

was large. However, as cover depth increased, both curves experienced the same trend, and the CS/HC decreased and gradually tended to a constant under enough depth.

4.2. Regression Analysis between Deformation and Cover Depth at 12.26 m Span

4.2.1. Linear Regression between CS and Cover Depth at 12.26 m Span. Figure 10 shows the scatter plot between CS and cover depth at 12.26 m span. It demonstrated that the CS increased as the cover depth increased. Considering the linear trend, the linear correlation coefficient was 0.622, and the regression equation is as follows:

$$y_{CS} = (2.222x - 83.490) \times 10^{-3}. \quad (5)$$

t-test was used for hypothesis testing H_0: $\beta_1 = 0$. The results were $t^* = 4.625 > t\ (0.05) = 2.149$ and P value $= 0.047 < 0.05 = \alpha$. There was sufficient evidence at the 0.05 significance level to conclude that there was a linear relationship in the population between cover depth and CS.

As vertical joints being developed, the earth pressure in the loess stratum increased with the increasing cover depth and the deformation after excavation increased correspondingly.

4.2.2. Linear Regression between HC and Cover Depth at 12.26 m Span. Figure 11 shows the scatter plot between HC and cover depth at 15.2 m span. It showed that the HC

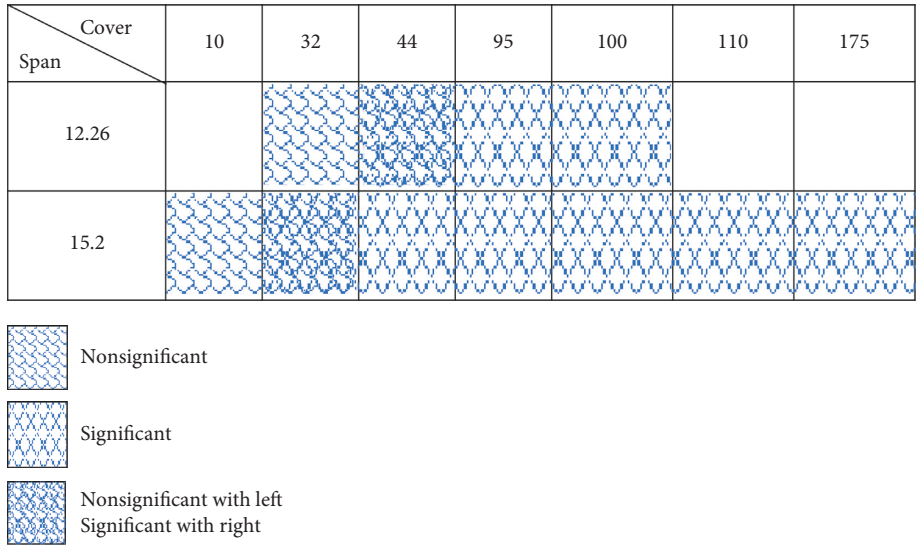

Figure 6: The results of ANOVA.

Table 4: ANOVA of deformation with different cover depth levels.

Span	Cover depth levers	F	F crit	P	Significance
CS					
12.2	32, 45	0.77	10.13	0.445	Not sig.
	45, 100	8.12	5.12	0.019	Sig.
15.2	10, 32	1.13	4.96	0.312	Not sig.
	32, 95, 110, 175	17.74	2.99	≤0.001	Sig.
HC					
12.2	32, 45	0.18	6.61	0.668	Not sig.
	45, 100	14.98	4.96	0.003	Sig.
15.2	32, 95, 110, 175	34.63	3.03	≤0.001	Sig.

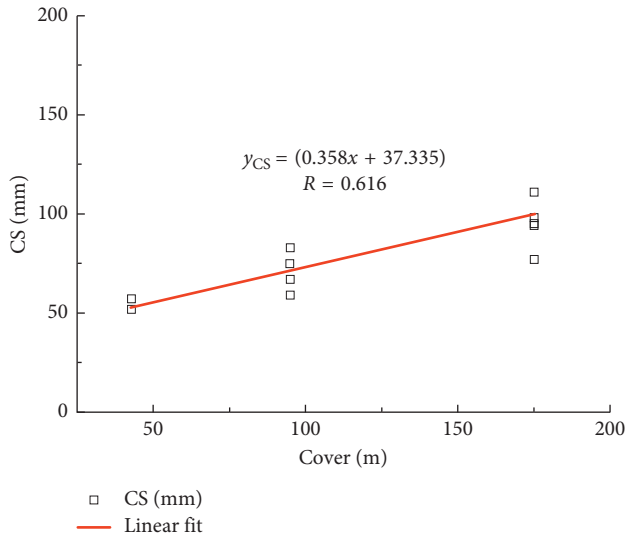

Figure 7: Linear regression between CS and cover depth at 15.2 m span.

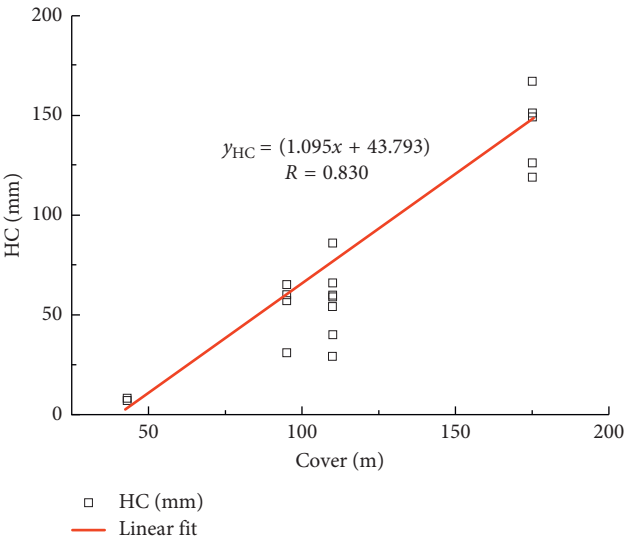

Figure 8: Linear regression between HC and cover depth at 15.2 m span.

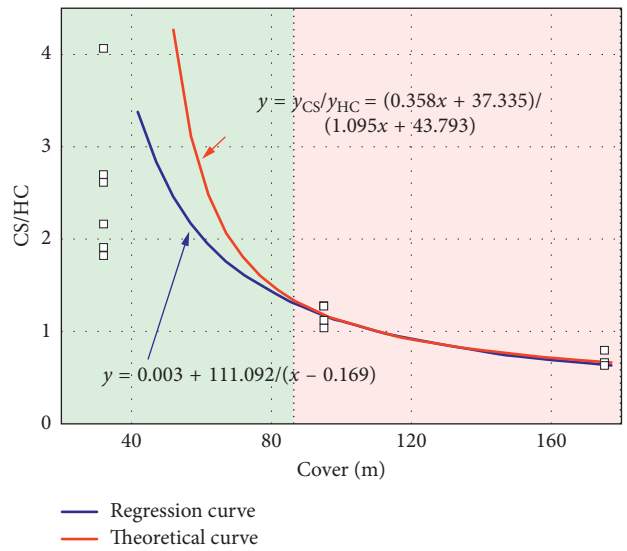

Figure 9: Comparison between theoretical curve and regression curve on relation of CS/HC with cover depth at 15.2 span. The graph of equation (3) was regarded as the theoretical curve, and the graph of equation (4) was regarded as the regression curve.

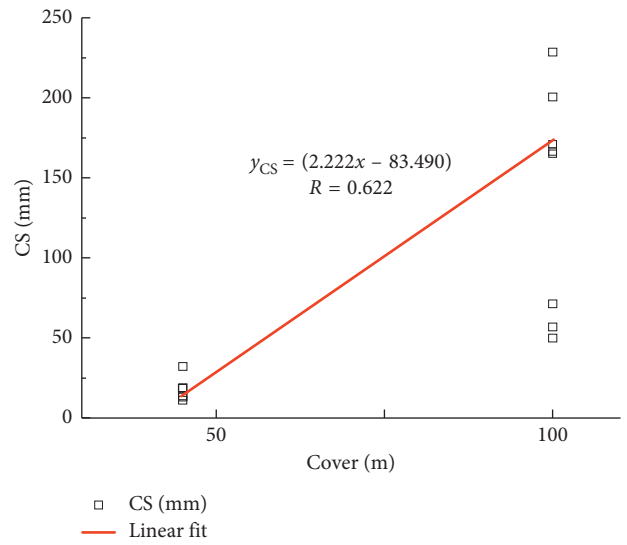

Figure 10: Linear regression between CS and cover depth at 12.26 span.

increased as the cover depth increased. Considering the linear trend, the linear correlation coefficient was 0.711, and the regression equation is as follows:

$$y_{HC} = (2.887x - 115.455) \times 10^{-3}. \quad (6)$$

t-test was used for hypothesis testing H_0: $\beta_1 = 0$. The results were $t^* = 6.280 > t\ (0.05) = 3.365$ and P value $= 0.004 < 0.05 = \alpha$. There was sufficient evidence at the 0.05 significance level to conclude that there was a linear relationship in the population between cover depth and HC.

4.2.3. Regression Analysis between CS/HC and Cover Depth at 12.26 m Span. To take in further analysis of the relation between deformation and cover depth, the characteristic of the data on the CS/HC from the on-site and the equation would be explored. The equation of the CS/HC varying with cover depth could be obtained by the fitting equation (5) CS and equation (6) HC. The new function is as follows:

$$y_T = \frac{y_{CS}}{y_{HC}} = \frac{(2.222x - 83.490)}{(2.887x - 115.455)}. \quad (7)$$

Equation (7) was fitted with the function being similar in the form of $y = a + b/(c + x)$. Nonlinear regression was carried out with SPSS software package, and the fitting equation was obtained as follows:

$$y_R = \frac{0.766 + 1.421}{(x - 43.829)}. \quad (8)$$

When the span was 12.26 m, the cover depth varied from 45 to 100 m, comparing the graph of equation (7) regarded as theoretical curve and equation (8) regarded as regression curve, and the result is plotted in Figure 12. When the cover depth was below 55 m, the difference between the two curves was large. However, as cover depth increased, both curves experienced the same trend and the CS/HC decreased and gradually tended to a constant under enough depth.

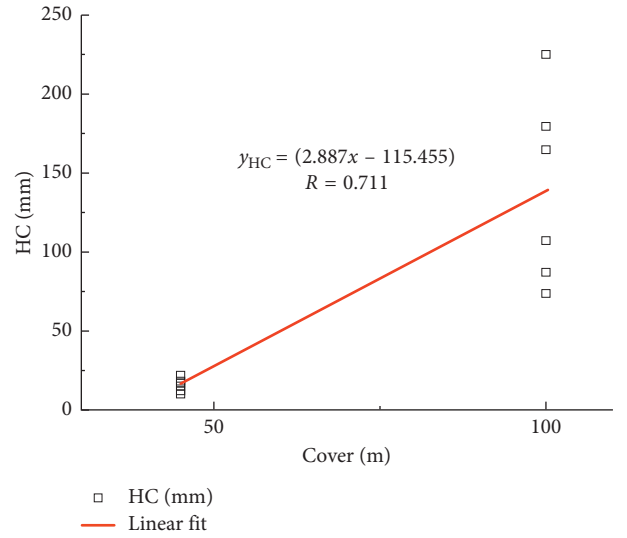

Figure 11: Linear regression between HC and cover depth at 12.26 m span.

4.3. Discussions on Regression Analysis. In the deep tunnel, as the cover depth increased, the deformation also increased, and the deformation had a linear function relationship with the cover depth. Figures 9 and 12 indicated that, with the increment of cover depth, the difference between theoretical curves and regression curves decreased. Hence, the function relationship was more applicable. However, with decrease in the cover depth, the difference between these two curves increased, and the function relationship between the cover depth and the deformation was gradually not applicable. The results further verified the randomness of deformation data in the shallow tunnel.

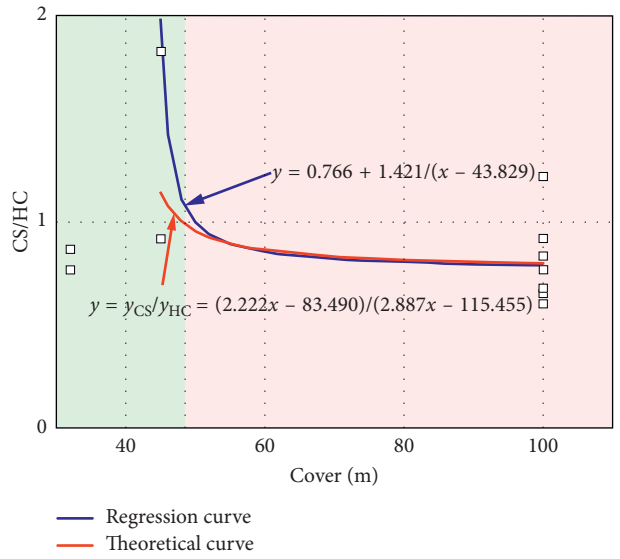

Figure 12: Comparison between theoretical curve and regression curve on relation of CS/HC with cover depth at 12.26 m span. The graph of equation (7) was regarded as the theoretical curve, and the graph of equation (8) was regarded as the regression curve.

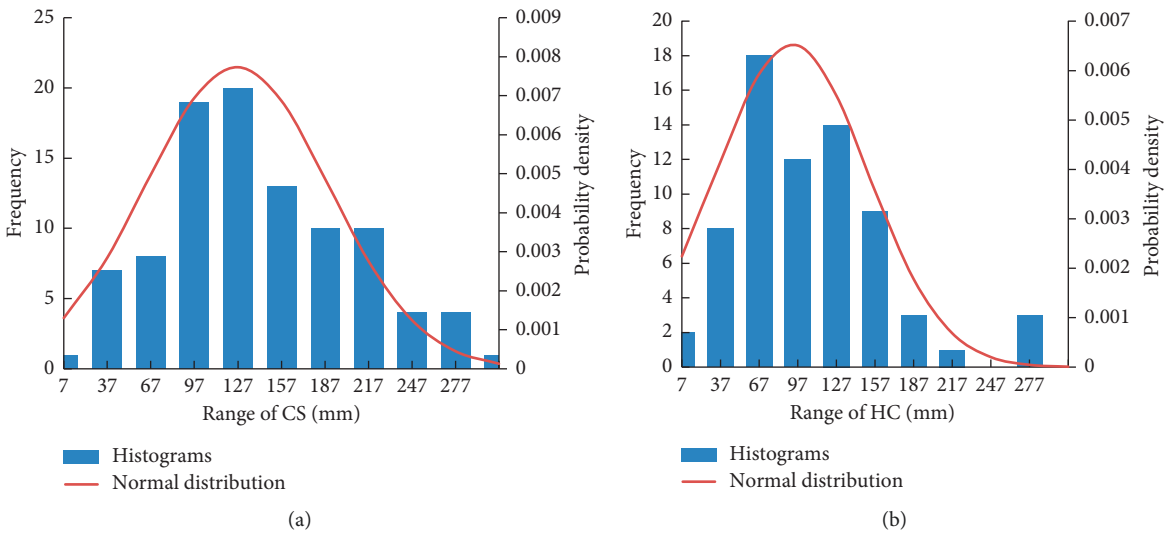

Figure 13: Histograms of tunnel deformation and normal distribution curve.

As loess has inherent strength, the vertical load of surrounding rock in the shallow tunnel was smaller than that in the deep one, and the vertical deformation was larger than the horizontal one. With the increase of tunnel depth, the soil pressure increased as well, and the initial stress was gradually dominated by tectonic stress, causing the increment of horizontal and vertical deformations [54–59]. Finally, horizontal and vertical deformations tended to be equal and CS/HC tends to be a constant.

5. Distribution of Deformation of the Shallow Tunnel

The data of loess tunnel deformation were discrete within 10 m to 30 m, and their histograms are described in Figure 13.

Figure 13 demonstrates that the tunnel deformation got close to a normal distribution in the shallow tunnel. One-sample Kolmogorov–Smirnov test was used for the normal distribution. For CS, $D_n = 0.088 < D_{97,0.05,} = 0.138$, Asymp. Sig. = 0.440 > 0.05, and the data of CS were a good fit with the normal distribution. Moreover, for HC, $D_n = 0.088 < D_{70,0.05,} = 0.163$, Asymp. Sig. = 0.547 > 0.05, and the data of HC were also a good fit with the normal distribution. Therefore, the descriptive parameters of the normal distribution could be used to study the regularity of deformation. The mean of CS was 105.4 mm, the standard deviation was 51.6 mm, and the coefficient of variance was 0.49. The mean of HC was 96.396 mm, the standard deviation was 61.139 mm, and the coefficient of variance was 0.63. There was a great discreteness in deformation data, 95% of CS data were within 190.3 mm, and 95% of HC data were less than 196.9 mm.

The horizontal and vertical deformations were mostly within 200 m in shallow tunnels. Therefore, the deformation allowance was recommended to be 200 mm.

6. Conclusions

(1) The influence of cover depth on deformation is significant in deep tunnels while is not significant in shallow tunnels. According to the difference of significance level on deformation between deep and shallow tunnels, a method defining the CDT in the tunnel by statistical methods is put forward by investigating whether the influence of tunnel depth on the deformation of surrounding rock is significant or not.

(2) In the deep tunnel, the deformation increases with the increase of cover depth, and the deformation has a linear function relationship with the cover depth. With the increment of cover depth, the CS/HC decreases and gradually tends to be a constant.

(3) In the cover depth of 10 to 30 m, the data of loess tunnel deformation are discrete and get close to a normal distribution. And the CS is mostly within 190.3 mm, and the HC is 196.9 mm. The amount of deformation in the loess tunnel is larger than that of in the rock tunnel, and the reserved deformation should be increased in tunnel design.

(4) The conclusion of statistical analyses can provide the statistical characteristics of the parameters of the random variables of tunnel surrounding rock for engineering reliability analysis. Variable parameter is the important support for probability design, and probability design is the development direction of tunnel and underground structures.

Data Availability

The data used to support the findings of this study are available from the corresponding author upon request.

Conflicts of Interest

The authors declare that they have no conflicts of interest.

Acknowledgments

This work was financially supported by the Science and Technology Project Plan of Traffic Construction in the West of China (Nos. 2001 318 000 21, 2007 318 000 18, and 2014 318 J27 210), the Brainstorm Project on Social Development of Shaanxi Provincial Science and Technology Department (No. 2016SF-412), and National Key R&D Program of China (No. 2017YFC0805306).

References

[1] Y. Li, Y. Song, L. Yan, T. Chen, and Z. An, "Timing and spatial distribution of loess in Xinjiang, NW China," *PLoS One*, vol. 10, no. 5, Article ID e0125492, 2015.

[2] H. Yu, C. Cai, A. Bobet, X. Zhao, and Y. Yuan, "Analytical solution for longitudinal bending stiffness of shield tunnels," *Tunnelling and Underground Space Technology*, vol. 83, pp. 27–34, 2019.

[3] X. Luo, D. Li, and S. Zhang, "Traffic flow prediction in holidays based on DFT and SVR," *Journal of Sensors*, vol. 2019, Article ID 6461450, 9 pages, 2019.

[4] T. Tan, "Fundamental properties of loess from Northwestern China," *Engineering Geology*, vol. 25, no. 2–4, pp. 103–122, 1988.

[5] Z. G. Lin and S. J. Wang, "Collapsibility and deformation characteristics of deep-seated loess in China," *Engineering Geology*, vol. 25, no. 2–4, pp. 271–282, 1988.

[6] A. M. Assallay, C. D. F. Rogers, and I. J. Smalley, "formation and collapse of metastable particle packings and open structures in loess deposits," *Engineering Geology*, vol. 48, no. 1–2, pp. 101–115, 1997.

[7] T. A. Dijkstra, "Geotechnical thresholds in the Lanzhou loess of China," *Quaternary International*, vol. 76-77, pp. 21–28, 2001.

[8] T. X. Zhu, "Gully and tunnel erosion in the hilly Loess Plateau region, China," *Geomorphology*, vol. 153-154, pp. 144–155, 2012.

[9] B.-P. Wen and Y.-J. Yan, "Influence of structure on shear characteristics of the unsaturated loess in Lanzhou, China," *Engineering Geology*, vol. 168, pp. 46–58, 2014.

[10] J. Zhao and C. Huang, "Progress of loess research in China," *Journal of Geographical Sciences*, vol. 4, no. 1, pp. 57–61, 2004.

[11] E. Derbyshire, X. Meng, and R. A. Kemp, "Provenance, transport and characteristics of modern aeolian dust in western Gansu Province, China, and interpretation of the quaternary loess record," *Journal of Arid Environments*, vol. 39, no. 3, pp. 497–516, 1998.

[12] I. J. Smalley and V. Smalley, "Loess material and loess deposits: formation, distribution and consequences," *Developments in Sedimentology*, vol. 38, pp. 51–68, 1983.

[13] H. Yu, Y. Yang, and Y. Yuan, "Analytical solution for a finite Euler-Bernoulli beam with single discontinuity in section under arbitrary dynamic loads," *Applied Mathematical Modelling*, vol. 60, pp. 571–580, 2018.

[14] Z. Q. Zhang, H. Zhang, Y. T Tan, and H. Y. Yang, "Natural wind utilization in the vertical shaft of a super-long highway tunnel and its energy saving effect," *Building and Environment*, vol. 145, pp. 140–152, 2018.

[15] S.-J. Feng, F.-L. Du, Z.-M. Shi, W.-H. Shui, and K. Tan, "Field study on the reinforcement of collapsible loess using dynamic compaction," *Engineering Geology*, vol. 185, pp. 105–115, 2015.

[16] H. Yu, Z. Zhang, J. Chen, A. Bobet, M. Zhao, and Y. Yuan, "Analytical solution for longitudinal seismic response of tunnel liners with sharp stiffness transition," *Tunnelling and Underground Space Technology*, vol. 77, pp. 103–114, 2018.

[17] J. Wang, Q. Huo, Z. Song, and Y. Zhang, "Study on adaptability of primary support arch cover method for large-span embedded tunnels in the upper-soft lower-hard stratum," *Advances in Mechanical Engineering*, 2019, In press.

[18] J. Golser, "The New Austrian tunnelling method (NATM), theoretical background and practical experiences," in *Proceedings of 2nd Shotcrete Conference*, Easton, PA, USA, October 1976.

[19] de M. M. Farias, Á. H. Moraes, and de A. P. Assis, "Displacement control in tunnels excavated by the NATM: 3-D numerical simulations," *Tunnelling and Underground Space Technology*, vol. 19, no. 3, pp. 283–293, 2004.

[20] J. Lai, J. Qiu, H. Fan et al., "Fiber bragg grating sensors-based in situ monitoring and safety assessment of loess tunnel," *Journal of Sensors*, vol. 2016, Article ID 8658290, 10 pages, 2016.

[21] J. Lai, K. Wang, J. Qiu, F. Niu, J. Wang, and J. Chen, "Vibration response characteristics of the cross tunnel structure," *Shock and Vibration*, vol. 2016, Article ID 9524206, 16 pages, 2016.

[22] J. Wang, Z. Ren, Z. Song, R. Huo, and T. Yang, "Study of the effect of micro-pore characteristics and saturation degree on the longitudinal wave velocity of sandstone," *Arabian Journal of Geosciences*, 2019, In press.

[23] S. Li, H. Wang, Y. Li, Q. Li, B. Zhang, and H. Zhu, "A new mini-grating absolute displacement measuring system for static and dynamic geomechanical model tests," *Measurement*, vol. 105, pp. 25–33, 2017.

[24] Y. Luo, J. Chen, S. Gao et al., "Stability analysis of super-large-section tunnel in loess ground considering water infiltration caused by irrigation," *Environmental Earth Sciences*, vol. 76, no. 22, p. 763, 2017.

[25] J. Qiu, H. Liu, J. Lai, H. Lai, J. Chen, and K. Wang, "Investigating the long term settlement of a tunnel built over improved loessial foundation soil using jet grouting technique," *Journal of Performance of Constructed Facilities*, vol. 32, no. 5, article 04018066, 2018.

[26] P. Li, Y. Zhao, and X. Zhou, "Displacement characteristics of high-speed railway tunnel construction in loess ground by using multi-step excavation method," *Tunnelling and Underground Space Technology*, vol. 51, pp. 41–55, 2016.

[27] V. Kontogianni, P. Psimoulis, and S. Stiros, "What is the contribution of time-dependent deformation in tunnel convergence?," *Engineering Geology*, vol. 82, no. 4, pp. 264–267, 2006.

[28] P. Li and Y. Zhao, "Performance of a multi-face tunnel excavated in loess ground based on field monitoring and numerical modeling," *Arabian Journal of Geosciences*, vol. 9, no. 14, 2016.

[29] Y. Li, X. Jin, Z. Lv, J. Dong, and J. Guo, "Deformation and mechanical characteristics of tunnel lining in tunnel intersection between subway station tunnel and construction tunnel," *Tunnelling and Underground Space Technology*, vol. 56, pp. 22–33, 2016.

[30] Z. Zhang, X. Shi, B. Wang, and H. Li, "Stability of NATM tunnel faces in soft surrounding rocks," *Computers and Geotechnics*, vol. 96, pp. 90–102, 2018.

[31] Z. J. Zhou, C. N. Ren, G. J. Xu, H. C. Zhan, and T. Liu, "Dynamic failure mode and dynamic response of high slope using shaking table test," *Shock and Vibration*, vol. 2019, Article ID 4802740, 15 pages, 2019.

[32] P. Li, F. Wang, and Q. Fang, "Undrained analysis of ground reaction curves for deep tunnels in saturated ground considering the effect of ground reinforcement," *Tunnelling and Underground Space Technology*, vol. 71, pp. 579–590, 2018.

[33] Z. Wang, J. S. Shen, and W. C. Cheng, "Simple method to predict ground displacements caused by installing horizontal jet-grouting columns," *Mathematical Problems in Engineering*, vol. 2018, Article ID 1897394, 11 pages, 2018.

[34] Y. Li, Y. Yang, H.-S. Yu, and G. Roberts, "Principal stress rotation under bidirectional simple shear loadings," *KSCE Journal of Civil Engineering*, vol. 22, no. 5, pp. 1651–1660, 2017.

[35] Z.-F. Wang, W.-C. Cheng, and Y.-Q. Wang, "Investigation into geohazards during urbanization process of Xi'an, China," *Natural Hazards*, vol. 92, no. 3, pp. 1937–1953, 2018.

[36] Z. Hu, "The Statistics Regulation on Pressure and Deformation of Surrounding Rock in Loess Tunnel," Master Thesis, Chang'an University, Xi'an, China, 2015, in Chinese.

[37] I. F. Jefferson, D. Evstatiev, D. Karastanev, N. G. Mavlyanova, and I. J. Smalley, "Engineering geology of loess and loess-like deposits: a commentary on the Russian literature," *Engineering Geology*, vol. 68, no. 3-4, pp. 333–351, 2003.

[38] I. F. Jefferson, N. Mavlyanova, K. O'Hara-Dhand, and I. J. Smalley, "The engineering geology of loess ground: 15 tasks for investigators-the mavlyanov programme of loess research," *Engineering Geology*, vol. 74, no. 1–2, pp. 33–37, 2004.

[39] Q. Yan, W. Zhang, C. Zhang, H. Chen, Y. Dai, and H. Zhou, "Back analysis of water and earth loads on shield tunnel and structure ultimate limit state assessment: a case study," *Arabian Journal for Science and Engineering*, 2018.

[40] Q. Liang, J. Li, X. Wu, and A. Zhou, "Anisotropy of Q2 loess in the Baijiapo tunnel on the lanyu Railway, China," *Bulletin of Engineering Geology and the Environment*, vol. 75, no. 1, pp. 109–124, 2015.

[41] China Merchants Chongqing Communications Technology Research and Design Institute CO., LTD, *Code for Design of Road Tunnel (JTG D70-2004)*, People's Communications Press, Beijing, China, 2004, in Chinese.

[42] Y. Li, S. Xu, H. Liu, E. Ma, and L. Wang, "Displacement and stress characteristics of tunnel foundation in collapsible loess ground reinforced by jet grouting columns," *Advances in Civil Engineering*, vol. 2018, Article ID 2352174, 16 pages, 2018.

[43] Z. Wang, Z. Hu, J. Lai, H. Wang, K. Wang, and W. Zan, "Settlement characteristics of jacked box tunneling underneath a highway embankment," *Journal of Performance of Constructed Facilities*, vol. 33, no. 2, pp. 1–12, 2019.

[44] Z. Wang, Y. Xie, H. Liu, and Z. Feng, "Analysis on deformation and structural safety of a novel concrete-filled steel tube support system in loess tunnel," *European Journal of Environmental and Civil Engineering*, 2018, In press.

[45] Y.-Q. Wang, Z.-F. Wang, and W.-C. Cheng, "A review on land subsidence caused by groundwater withdrawal in Xi'an, China," *Bulletin of Engineering Geology and the Environment*, 2018.

[46] H. Yu, X. Yan, A. Bobet, Y. Yuan, G. Xu, and Q. Su, "Multi-point shaking table test of a long tunnel subjected to non-uniform seismic loadings," *Bulletin of Earthquake Engineering*, vol. 16, no. 2, pp. 1041–1059, 2017.

[47] R. Qiao, Z. Shao, W. Wei, and Y. Zhang, "Theoretical investigation into the thermo-mechanical behaviours of tunnel lining during RABT fire development," *Arabian Journal for Science and Engineering*, vol. 44, pp. 1–12, 2019.

[48] R. J. Qiao, Z. S. Shao, F. Y. Liu, and W. Wei, "Damage evolution and safety assessment of tunnel lining subjected to long-duration fire," *Tunnelling and Underground Space Technology*, vol. 83, pp. 354–363, 2019, In press.

[49] Y. W. Zhang, X. L. Weng, Z. P. Song, and Y. F. Sun, "Modeling of loess soaking induced impacts on metro tunnel using water soaking system in centrifuge," *Geofluids*, vol. 2019, Article ID 5487952, 13 pages, 2019.

[50] H. J. Zhang, Z. Z. Wang, F. Lu, G. Y. Xu, and W. G. Qiu, "Analysis of the displacement increment induced by removing temporary linings and corresponding countermeasures," *Tunnelling and Underground Space Technology*, vol. 73, pp. 236–243, 2018.

[51] Y. Zhao, G. Li, and Y. Yu, *Loess Tunnel Engineering*, ISBN 9787113138370, China Railway Publishing House, Beijing, China, 2011, in Chinese.

[52] C. Liu, Z. Fan, X. Chen et al., "Experimental study on bond behavior between section steel and RAC under full replacement ratio," *KSCE Journal of Civil Engineering*, 2018, In press.

[53] C. Liu, Z. Lv, C. Zhu et al., "Study on calculation method of long term deformation of RAC beam based on creep adjustment coefficient," *KSCE Journal of Civil Engineering*, vol. 23, no. 1, pp. 260–267, 2019.

[54] Q. Yan, H. Chen, W. Chen, J. Zhang, S. Ma, and X. Huang, "Dynamic characteristic and fatigue accumulative damage of a cross shield tunnel structure under vibration load," *Shock and vibration*, vol. 2018, Article ID 9525680, 14 pages, 2018.

[55] Q. P. Wang and H. Sun, "Traffic structure optimization in historic districts based on green transportation and sustainable development concept," *Advances in Civil Engineering*, vol. 2019, Article ID 9196263, 16 pages, 2019.

[56] X. Nie, X. Wei, X. Li, and C. Lu, "Heat treatment and ventilation optimization in a deep mine," *Advances in Civil Engineering*, vol. 2018, Article ID 1529490, 12 pages, 2018.

[57] R. Ren, H. Zhou, Z. Hu, S. He, and X. Wang, "Statistical analysis of fire accidents in Chinese highway tunnels 2000–2016," *Tunnelling and Underground Space Technology*, vol. 83, pp. 452–460, 2019.

[58] X. Z. Li, X. L. Qu, C. Z. Qi, and Z. S. Shao, "A unified analytical method calculating brittle rocks deformation induced by crack growth," *International Journal of Rock Mechanics and Mining Sciences*, vol. 113, pp. 134–141, 2019.

[59] S. He, L. Su, H. Fan, and R. Ren, "Methane explosion accidents of tunnels in SW China," *Geomatics, Natural Hazards and Risk*, 2019, In press.